Gold clusters showing pentagonal atomic arrays revealed by aberration-corrected scanning transmission electron microscopy

Alvaro Mayoral,[a] Douglas A. Blom,[b] Marcelo M. Mariscal,[c] Claudia Guiterrez-Wing,[d] Juan Aspiazu,[d] Miguel Jose-Yacaman*[a]

Received (in XXX, XXX) Xth XXXXXXXXX 200X, Accepted Xth XXXXXXXXX 200X
First published on the web Xth XXXXXXXXX 200X
DOI: 10.1039/b000000x

In this work we present the analysis by aberration corrected electron microscopy of the formation of gold clusters based on the proton irradiation of larger nanoparticles (NP). Pentagonal arrays have been observed and energetic calculations have been performed in order to prove the stability of these materials.

In recent years noble metals clusters, such as gold or silver, have attracted extraordinary attention[1, 2] due to their high reactivity. Potential applications[2, 3] in the fields of catalysis and nanoelectronics are currently being explored in both theoretical and experimental ways to finally fabricate materials with tunable structures and properties on the nanometer scale. These properties are strongly related to the size and shape of the clusters[4] and in the particular case of gold, relativistic effects cause Au_n clusters to present unique structures and properties relative to the other "noble" metals. Many structures for different cluster sizes have been theoretically predicted[5, 6]; planar symmetries (2D) have been reported for clusters up to about 11–13 atoms. Three-dimensional morphologies are energetically preferred for larger clusters[7, 8]. Tetrahedral morphology has found to stabilize Au_{20}[9, 10]. Meanwhile, for larger clusters such as Au_{32}, Au_{42} or Au_{72}, hollow structures tend to present the lowest energy[11-14]; Moreover, cage structures (23 to 42 atoms) are energetically stable on MgO surfaces[15]. Unfortunately, due to the small size of these solids, little is known from the experimental point of view[16]. With the development of aberration corrected transmission electron microscopes, atomic resolution can be achieved and therefore, smaller materials which are 'not visible' by conventional electron microscopy techniques can be directly imaged[16, 17].

The analysis carried out in this work was mainly done using the STEM-HAADF technique. In this mode heavy elements such as metals appear very bright respect to light elements such as carbon. However, until the introduction of these machines the analysis of small nanoparticles was practically impossible as the probe size tended to be larger than the interatomic distances. With the implementation of aberration correctors[17-19] in STEM microscopes, electron probes smaller than 1 Å have been achieved, allowing dynamic imaging of single atoms and clusters composed of a few atoms. In this work gold nanoparticles, which were deposited onto a fine layer of graphite, were irradiated with a proton beam for up to 500 hours. Following irradiation, small gold clusters, as well as, isolated gold atoms were observed. The materials obtained were characterized by aberration corrected transmission electron microscopy, which allows observing in great detail isolated gold atoms, small clusters with sizes below 1 nm and the structure of larger nanoparticles of about 2nm[16, 20, 21]. These NP were found to be quite stable under electron beam irradiation retaining the *fcc* structure of bulk gold.

Producing clusters in the range below 1 nm is extraordinary difficult because if "bare" surface particles are formed, very strong cluster mobility is expected which would result in coalescence. The production of such small particles was carried out as follows: gold nanoparticles passivated with 1-dodecanethiol were synthesized by the Brust method reported elsewhere[22, 23]. 3 mg of the passivated gold nanoparticles were mixed with 100 mg of graphite in 0.5 ml of toluene and then mounted over a brass sample holder. The solvent was allowed to evaporate until a dry pellet of the sample was formed. The samples were irradiated in an EN Tandem Van de Graaff accelerator, with a proton beam of 5 MeV and a total dose of 2.4×10^8 Gy for periods of time ranging from 100 to 500 hours.

Scanning transmission electron microscopy (STEM) was used to image the materials in a JEOL 2100F 200kV FEG-STEM/TEM equipped with a CEOS C_s corrector on the illumination system. High angle annular dark-field (HAADF) STEM images were acquired on a Fischione Model 3000 HAADF detector with a camera length such that the inner cut-off angle of the detector was 50 mrad. The pixel spacing was calibrated using Si 110 lattice images in HAADF mode.

High resolution STEM images were processed using the Richardson-Lucy algorithm implemented by Ichizuka[24]. The possibility of misinterpretation of the filtered images by the introduction of artefacts was ruled out by the analysis of several image of larger particles and isolated atoms.

Theoretical calculations were performed within a DFT-LDA pseudopotential framework using the DMOL3 code[25]. Effective core potentials were used for carbon and gold atoms, including semi-relativistic effects. All electron calculations were carried out with a double numeric plus polarization basis set. The local density approximation (LDA) within the Perdew-Wang (PWC) functional were used in all cases.

Fig. 1a shows the bright field image of a hexagonal shaped Au NP of about 3 nm. The lattice distances measured are 2.75 Å, which correspond to the double distance for the {110} planes in a *fcc* structure obtaining a unit cell value of 3.89 Å, smaller than the data reported for bulk Au (4.07 Å). This apparent lattice decrease has been previously reported for gold nanoparticles below 3nm[21]. As described in the experimental section, the original gold nanoparticles were irradiated until

they split into smaller fractions which remained deposited on the carbon. Fig. 1b shows a 'large' gold nanoparticle of ~ 2.5 nm recorded along the [110] orientation in the process of disintegration; two smaller clusters of ~ 1 nm, which have been created due to the irradiation are still linked (marked with a circle in Fig. 1b) to the 'parental' nanoparticle.

Fig. 2 displays several single Au atoms on the carbon. The full-width half maximum of the intensity measured after black level correction (performed by subtracting the intensity measured on gold atoms and clusters minus the intensity measured on empties zones) was 1.03 in agreement with data previously reported[17, 26, 27] for isolated metal atoms on carbon. Considering that the diffusion barrier for a gold adatom on a graphene sheet is 0.05 eV[28] a high atomic mobility is expected for Au adatoms on defect-free graphene sheets. However, if it is taken into account the possibility of Au adatoms adsorbed on graphene vacancies, which may be created due to proton irradiation, the diffusion barriers change drastically to the order of 2.2 and 5 eV, indicating that gold atoms could be trapped on carbon vacancies or will migrate together with the vacancies as predicted very recently by Zhang *et. al.*[29].

Fig. 3 presents the STEM-HAADF images of two different gold clusters. Fig. 3a corresponds to a cluster of less than 1nm, composed by approximately 17-18 atoms, with planar morphology. A pentagonal array of gold atoms is marked by an arrow. In Fig. 3b an isolated pentagon is presented. Fig. 4a displays another gold cluster of ~ 12 Å, composed by ~ < 50 atoms, where an almost completely flat pentagonal array is highlighted in Fig. 4b. In this case the atomic distances between the gold atoms forming the pentagon varied from 2.1 Å to 2.6 Å. The intensity profile line of this particle, (obtained from the raw data), is shown in the suplementary material compared with the result obtained for a single atom.

All the images were recorded for either 16 or 20 seconds; during this time, no structural changes were observed in the atomic structure of the clusters proving that the pentagonal arrays were formed and stabilized after the proton irradiation. However, for longer exposure times, the interaction between the electron beam and the gold became predominant over the interaction between the Au atoms and the carbon substrate making the cluster mobile over the surface of the graphite. Theoretical calculations have been performed using free and supported Au clusters: *Free Au_5 clusters:* First, we started the calculations with small free clusters composed of five gold atoms in a 3-dimensional array (Fig. 5a). Geometry optimizations revealed a planar 2D-structure in good agreement with previous studies[30]. Au_5 presents a planar trapezoidal structure (Fig. 5b) with a C_2v symmetry which is more stable than the 3D by 1.45 eV. *Supported Au_5 clusters:* The systems considered include two graphene layers within a 5 × 5 unit cell and the optimized Au_5 cluster (Fig. 5b) onto the surface. During these calculations the first atomic layer of graphite and all gold atoms were allow to relax. Geometry optimization were performed and the final structure obtained after relaxation is shown in Fig. 5c. The calculations show that gold atoms are placed above C-C bonds with a slight displacement towards the hollow site, the Au-Au distances are in the range of 2.62–2.71 Å as indicated in the figure. Although the structure is not exactly the same as in Fig. 4b, it is in fairly agreement with the experimental findings, especially considering that the calculations are predictions at 0 K.

The presence of pentagonal arrays of atoms is extremely important; suggesting that a five fold related structure is present. No *fcc* structure would produce such an array of atoms except if a star disclination is produced deforming the structure to a five fold structure. However, this would not produce pentagons as presented in this work. Theoretically, for such a small materials gold fullerenes have been energetically predicted to be the most stable phase. The stability has been attributed to their spherical aromaticity following the $2(N + 1)^2$ rule[31, 32]. Good examples are Au_{50} and Au_{72}, which have been found to be stable and form fullerene type geometry[13, 33, 34]. To date, hollow Au_{32} has only been successfully prepared via immersion in an organic ligand[35], but experimental evidence has not been recorded from the electron microscopy point of view. In the present work pentagonal arrays, which to our knowledge are reported for the first time have been produced and analyzed, and could represent an experimental evidence of a precursor for the fullerene-like morphologies.

Conclusions

In summary, a method for the production of gold clusters based on the proton irradiation of larger crystals has been described which creates isolated gold atoms and small nanoparticles of different sizes, which were characterized by BF-STEM and HAADF-STEM.

Gold clusters smaller than 1nm have been successfully synthesized presenting in some cases a structure with pentagonal arrays.

The authors would like to thank NSF grant award DMR-0830074: ''Alloys at the Nanoscale: The Case of Nanoparticles''. We also recognize CONACYT and CONICET for funding and D. Olmos for technical support.

Notes and references

[*a] *Department of Physics and Astronomy The University of Texas at San Antonio. One UTSA Circle, San Antonio, TX78249 USA; E-mail: miguel.yacaman@utsa.edu*

[b] *EM Center University of South Carolina 715 Sumter St. Coker Life Sciences 001 Columbia, SC 29208, USA*

[c] *INFIQC/CONICET Universidad Nacional de Córdoba, Facultad de Ciencias Químicas, Departamento de Matemática y Física. Haya de la Torre y Medina Allende. Cdad Universitaria. X5000HUA Córdoba, Argentina.*

[d] *Instituto Nacional de Investigaciones Nucleares Carretera México-Toluca S/N, La Marquesa Ocoyoacac, Estado de México, C. P. 52750, MEXICO*

† Electronic Supplementary Information (ESI) available: [details of any supplementary information available should be included here]. See DOI: 10.1039/b000000x/

1. R. E. Smalley, *Acc. Chem. Res.*, 1992, **25**, 98.
2. P. Schwerdtfeger, *Angew. Chem. Int. Ed.*, 2003, **42**, 1892.
3. A. S. K. Hashmi and G. J. Hutchings, *Angew. Chem. Int. Ed.*, 2006, **45**, 7896.
4. M. S. Chen and D. W. Goodman, *Catal. Today*, 2006, **22**, 111.

5. M. J. Yacaman, J. A. Asencio, H. B. Liu and J. Gardea-Torresdey, *J. Vac. Sci. Technol.*, 2001, **19**, 1091.
6. K. Koga and H. Takeo, *Phys. Rev. B*, 1998, **57**, 4053.
7. S. Bulusu, X. Li, L.-S. Wang and X. C. Zeng, *Proc. Natl. Acad. Sci.*, 2006, **103**, 8326.
8. S. Bulusu and X. C. Zeng, *J. Chem. Phys.*, 2006, **125**, 154303.
9. J. Li, X. Li, H.-J. Zhai and L.-S. Wang, *Science*, 2003, **299**, 864.
10. M. P. Johansson and P. Pyykkö, *Phys. Chem. Chem. Phys.*, 2004, **6**, 2907.
11. M. Ji, X. Gu, X. Li, X. Gong, J. Li and L.-S. Wang, *Angew. Chem. Int. Ed.*, 2005, **44**, 7119.
12. Y. Gao and X. C. Zeng, *J. Am. Chem. Soc.*, 2005, **127**, 3698.
13. A. J. Karttunen, M. Linnolahti, T. A. Pakkanen and P. Pyykkö, *Chem. Commun.*, 2008, 465-467.
14. M. P. Johansson, J. Vaara and D. Sundholm, *J. Phys. Chem. C*, 2008, **112**, 19311.
15. R. Ferrando, G. Barcaro and A. Fortunelli, *Phys. Rev. Lett.*, 2009, **102**, 216102.
16. Z. Y. Li, N. P. Young, M. D. Vece, S. Palomba, R. E. Palmer, A. L. Bleloch, B. C. Curley, R. L. Johnston, J. Jiang and J. Yuan, *Nature*, 2008, **451**, 46.
17. P. E. Baston, N. Dellby and O. L. Krivanek, *Nature*, 2002, **418**, 617.
18. O. L. Krivanek, N. Delby and A. R. Lupini, *Ultramicroscopy*, 1999, **78**, 1.
19. M. Haider, S. Uhlemann and J. Zach, *Ultramicroscopy*, 2000, **81**, 163.
20. E. P. W. Ward, I. Arslan, P. A. Midgley, A. Bleloch and J. M. Thomas, *Chem. Commun.*, 2005, **5805**.
21. L. F. Allard, A. Borisevich, W. Deng, R. Si, M. Flytzani-Stephanopoulos and S. H. Overbury, *Journal of Electron Microscopy*, 2009, **58**, 199.
22. M. Brust, M. Walker, D. Bethell, D. J. Schiffrin and R. J. Whyman, *J. Chem. Soc. Chem. Commun.*, 1994, 801.
23. C. Gutiérrez-Wing, P. Santiago, J. A. Ascencio, A. Camacho and M. José-Yacamán, *Appl. Phys. A*, 2000, **71**, 237.
24. D. i. c. a. f. H. R. I. (www.hremresearch.com).
25. B. Delley, *J. Chem. Phys.*, 2000, **113**, 7756-7764.
26. P. E. Baston, *Ultramicroscopy*, 2006, **106**, 1104.
27. D. A. Blom, L. A. Allard, S. Mishina and M. A. O'Keefe, *Microscopy and Microanalisys* 2006, **12**, 483.
28. P. Jensen, X. Blase and P. Ordejón, *Surf. Sci.*, 2004, **564**, 173.
29. W. Zhang, L. Sun, Z. Xu, A. V. Krasheninnikov, P. Huai, Z. Zhu and F. Banhart, *Phys. Rev. B*, 2010, **81**, 125425.
30. P. K. Jain, *Struct. Chem.*, 2005, **16**, 421.
31. M. P. Johansson, D. Sundholm and J. Vaara, *Angew. Chem. Int. Ed.*, 2004, **43**, 2678.
32. A. Hirsch, Z. Chen and H. Jiao, *Angew. Chem. Int. Ed.*, 2000, **39**, 3915.
33. J. Wang, J. Jellinek, J. Zhao, Z. Chen, R. B. King and P. von-RaguéSchleyer, *J. Phys. Chem. A*, **109**, 9265.
34. D. Tian, J. Zhao, B. Wang and R. B. King, *J. Phys. Chem. A*, 2007, **111**, 411.
35. M. J. Oila and A. M. P. Koskinen, *ARKIVOC*, 2006, **15**, 76.

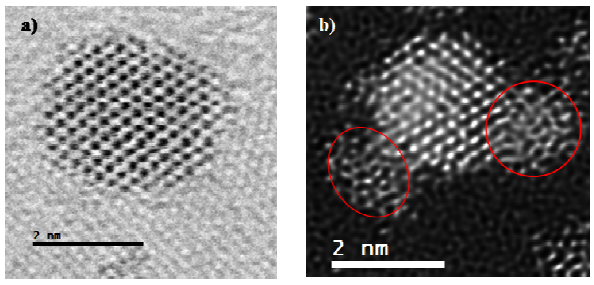

Fig. 1 a) Aberration corrected STEM-BF of a gold cluster, the gold atoms; in this case appear as black spots in the image.. b) High resolution STEM-HAADF image of a gold cluster recorded along [110] orientation after gamma irradiation. The circles remark two small clusters formed after irradiation.

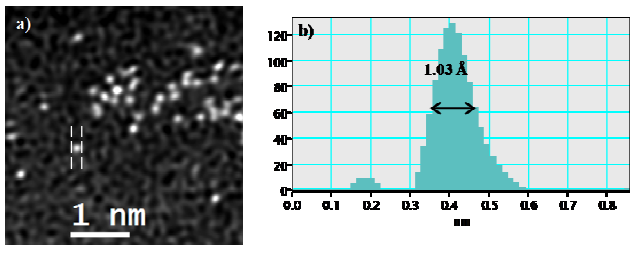

Fig. 2 High resolution STEM-HAADF image of single gold atoms deposited on a layer of graphite. The atom used in this case for diameter measurements is marked by two dashed lines.

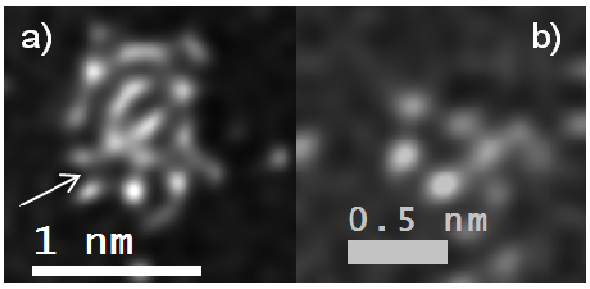

Fig. 3 a) Aberration corrected STEM-HAADF of a Au cluster. A pentagonal array is marked by an arrow. b) HR-STEM-HAADF image of a Au cluster formed by two pentagons.

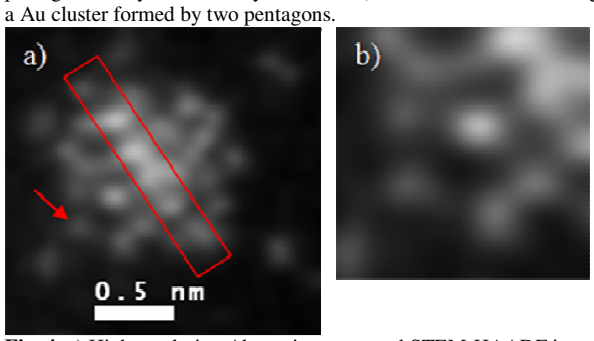

Fig. 4 a) High resolution Aberration corrected STEM-HAADF image of a gold cluster of about 1.2 nm. b) Pentagonal array collected from Fig. 4a. The distances between gold neighbours oscillated between 2.1 Å to 2.6 Å.

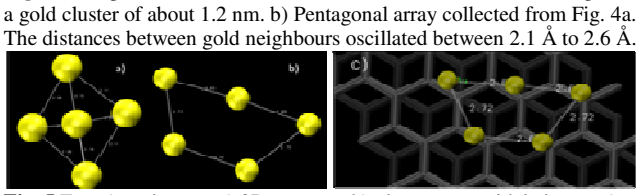

Fig. 5 Free Au_5 clusters: a) 3D structure b) planar trapezoidal cluster. c) Supported Au_5 cluster on graphite 5×5.